Isorhamnetin Attenuates Isoproterenol-Induced Myocardial Injury by Reducing ENO1 in Cardiomyocytes

Zhenli Guo , Shizhong Liu , Xianghong Hou , Xin Zhou , Yan Wang , Yi Rong , Rui Yang * , Xinzhi Li * , Ketao Ma *

Posted Date: 10 April 2025

doi: 10.20944/preprints202504.0915.v1

Keywords: isorhamnetin; isoprenaline; myocardial injury; ENO1; glycolysis; oxidative stress.

 doi:10.20944/preprints202504.0915.v1

Article

Isorhamnetin Attenuates Isoproterenol-Induced Myocardial Injury by Reducing ENO1 in Cardiomyocytes

Zhenli Guo [1,2,†], Shizhong Liu [1,2,†], Xianghong Hou [1,3], Xin Zhou [1,2], Yan Wang [1,2], Yi Rong [1,2], Rui Yang [1,2,*], Xinzhi Li [1,3,*] and Ketao Ma [1,2,*]

[1] The Key Laboratory of Xinjiang Endemic and Ethnic Diseases, Ministry of Education, Shihezi University Medical College, Shihezi 832002, China

[2] Department of Physiology, Shihezi University Medical College, Shihezi 832002, China

[3] Department of Pathophysiology, Shihezi University Medical College, Shihezi 832002, China

* Correspondence: 458360505@qq.com (R.Y.); lixinzhi@shzu.edu.cn (X.L.); maketao@shzu.edu.cn (K.M.); Tel: +86-15001645180 (K.M.)

† These authors contributed equally to this work.

Abstract: The protective effect of isorhamnetin on myocardial injury induced by isoproterenol (ISO) was investigated to identify key targets and pathways involved, offering potential therapeutic insights for cardiovascular diseases. The myocardial injury model was established through intraperitoneal ISO injection, and the effects of isorhamnetin on apoptosis and oxidative stress in ISO-induced myocardial injury rats were assessed. Additionally, an ISO-induced H9c2 cell injury model was established to evaluate the impact of isorhamnetin on cellular damage. Transcriptomic sequencing of H9c2 cells was conducted to identify differentially expressed genes, followed by gene enrichment analysis. Intracellular glucose, lactate, and ATP levels were quantified, and protein expression of key pathway targets ENO1, PPARα, and PGC-1α was analyzed via immunoblotting. Isorhamnetin improved cardiac dysfunction and morphological damage, reduced serum markers of cardiac injury, and exerted cardioprotective effects by regulating oxidative stress and inhibiting apoptosis. Compared to the ISO group, the glycolytic process, with ENO1 as a key target and the PPAR signaling pathway as the core regulator, was significantly suppressed in the isorhamnetin-pretreated group. Furthermore, isorhamnetin pretreatment reduced intracellular glucose and lactate levels while increasing ATP content in a concentration-dependent manner. These findings suggest that isorhamnetin protects the heart by inhibiting ENO1, activating the PPARα/PGC-1α signaling axis, reversing isoprenaline-induced metabolic shifts in H9c2 cells, suppressing glycolysis, and enhancing ATP release, thereby mitigating apoptosis and oxidative stress.

Keywords: isorhamnetin; isoprenaline; myocardial injury; ENO1; glycolysis; oxidative stress

1. Introduction

For nearly three decades, cardiovascular diseases (CVDs) have been the leading cause of global mortality [1]. Recent reports indicate that in 2021, CVDs were responsible for approximately 20.5 million deaths, accounting for nearly one-third of all global fatalities [2]. Despite advancements in heart failure management, readmission and mortality rates remain alarmingly high. Isoprenaline (ISO), a synthetic nonselective β-adrenergic agonist, exerts positive inotropic effects, yet, when administered in high doses, it can increase myocardial oxygen consumption and elevate myocardial injury markers, culminating in cardiac dysfunction [3]. Addressing ISO-induced cardiac dysfunction and exploring novel cardioprotective agents are of critical clinical significance.

Numerous studies suggest that ISO-induced myocardial damage is linked to various pathophysiological mechanisms, including mitochondrial dysfunction [4], apoptosis [5],

 doi:10.20944/preprints202504.0915.v1

inflammation [6], oxidative stress [7], and disrupted energy homeostasis [8]. ENO1, an oncoprotein located both on the cell surface and within the cytoplasm, has recently gained attention for its pivotal role in cardiac pathologies [9,10]. Ji et al. demonstrated that downregulation of ENO1 can suppress glycolysis, thereby reducing myocardial fibrosis after a heart attack [11]. However, the interplay between ENO1, apoptosis, and oxidative stress in cardiomyocytes during heart failure progression remains poorly understood.

As cardiovascular research advances, there has been a growing interest in the pharmacological and biological properties of compounds derived from traditional Chinese medicine [12]. Flavonoids, such as those found in sea buckthorn and ginkgo biloba, have received considerable attention for their therapeutic potential [13,14]. Among these, isorhamnetin stands out as a promising natural compound [15]. Recent studies have emphasized its diverse biological activities, including cardiovascular protection [16,17], anti-apoptotic effects [18], and antioxidant properties [19]. However, the capacity of isorhamnetin to mitigate ISO-induced myocardial damage by restoring energy metabolism through glycolysis inhibition remains unexplored, and its underlying mechanisms are not fully understood.

This study investigates the protective effects and molecular mechanisms of isorhamnetin against ISO-induced myocardial injury. The research utilized both in vivo models of ISO-induced heart injury and in vitro models of ISO-induced H9c2 myocardial cell damage, coupled with transcriptomic analysis, to provide a scientific foundation for the clinical application of therapeutic agents in the treatment of myocardial injury.

2. Materials and Methods

2.1. Materials

Isorhamnetin (Isor; B21554) was obtained from Shanghai Yuanye Biotechnology Co. (Shanghai, China). Isoproterenol hydrochloride (ISO; I5627) was purchased from Sigma-Aldrich (St. Louis, MO, USA). Primary antibodies for Bax (ab32503), Bcl-2 (ab182858), caspase-3 (ab184787), and ENO1 (ab227978) were sourced from Abcam (Cambridge, United Kingdom). Nrf2 (16396-1-AP), NQO1 (11451-1-AP), HO-1 (10701-1-AP), PPARα (66826-1-Ig), PGC-1α (66369-1-Ig), and β-actin (66009-1-Ig) antibodies were provided by Proteintech Biotechnology Co. (Wuhan, China). Secondary antibodies, goat anti-rabbit IgG (ZB-2306) and goat anti-mouse IgG (ZB-2305), were acquired from Zhong Shan-Golden Bridge Biological Technology Co. (Beijing, China). Kits for lactate dehydrogenase (LDH; A020-2-2), superoxide dismutase (SOD; A001-3-2), malondialdehyde (MDA; A003-1-2), glucose (GLU; F006-1-1), and lactic acid (LD; A019-2-1) were obtained from Nanjing Jiancheng Biotechnology Co. Ltd. (Nanjing, China). Creatine kinase isoenzyme (CK-MB; JL12296) and cardiac troponin I (cTnI; JL13014) kits were purchased from Shanghai Jianglai Industry Co. Ltd. (Shanghai, China). Cell viability was assessed using Cell Counting Kit 8 (CCK-8) detection kits from APExBIO Technology LLC (Shanghai, China). The Annexin V-FITC/PI Apoptosis Kit was procured from Multisciences Biotech Co. (Hangzhou, China). Dimethyl sulfoxide (DMSO), RIPA buffer, phenylmethylsulfonyl fluoride (PMSF), and an Oil Red O staining kit were purchased from Solarbio Science & Technology Co. Ltd. (Beijing, China).

2.2. Animals and Experimental Protocols

Male SD rats, weighing between 160 and 180 grams, were obtained from Henan Skobes Biotechnology Co. Ltd. The rats were housed in the Animal Experimental Feeding Center at Shihezi University, where appropriate living conditions were provided. All animal experiments and procedures were approved by the Institutional Animal Care and Use Committee of Shihezi University, in compliance with the university's ethical guidelines for animal experimentation. Myocardial injury was induced by intraperitoneal injection of ISO (85 mg/kg) on two consecutive days, with a 24-hour interval between doses. The rats were randomly assigned to five groups, each consisting of 8-10 animals, with the following treatment regimens:

 doi:10.20944/preprints202504.0915.v1

Control Group (Control): Normal saline was administered for nine consecutive days.

ISO Group (ISO): Rats were given saline for the first seven days, followed by ISO (85 mg/kg) on days eight and nine via intraperitoneal injections.

Isorhamnetin Low-Dose Group (ISO + Isor -L) and High-Dose Group (ISO + Isor -H): Isorhamnetin (5 mg/kg or 10 mg/kg) was administered intraperitoneally every 24 hours from Day 1 to Day 7, followed by ISO (85 mg/kg) on days eight and nine.

Propranolol Group (ISO + Pro): Propranolol was administered intraperitoneally at a dose of 10 mg/kg daily during the first week, with ISO (85 mg/kg) given on days eight and nine.

After a 24-hour period following the final dose of isorhamnetin and ISO, the rats were anesthetized, and their thoracic cavities were rapidly exposed. Blood was collected from the heart for analysis, and the heart was excised. A segment was fixed in 4% paraformaldehyde for paraffin embedding and sectioning, while the remaining tissue was homogenized for further tests.

2.3. Cell Culture and Treatments

H9c2 cells were obtained from the Cell Bank of the Chinese Academy of Sciences, Shanghai. These cells were cultured in DMEM supplemented with 10% fetal bovine serum and 1% penicillin-streptomycin. The cells were divided into several groups: a control group, an ISO group, and three ISO + Isor groups with concentrations of 1.25 μM, 2.5 μM, and 5 μM, respectively. In the experimental setup, H9c2 cells were treated with isorhamnetin for 2 hours, followed by exposure to ISO (140 μM) for 48 hours.

2.4. Cardiac Injury-Associated Enzymes

Terum was extracted from whole blood samples, and according to the protocol, reagent and serum samples were mixed. Absorbance was measured using a microplate reader to assess the enzymatic activity of cTnI and CK-MB.

2.5. Histopathological Study

Heart tissue was fixed in 4% paraformaldehyde, then embedded in paraffin and sectioned into 5 μm thick slices. These sections underwent H&E and Masson staining. Stained slices were analyzed and photographed under a light microscope.

2.6. Terminal Deoxynucleotidyl Transferase dUTP Nick end Labeling (TUNEL)

Cardiac tissue segments were subjected to TUNEL staining to detect apoptotic cells, following the manufacturer's instructions. The extent of myocardial cell death was quantified by calculating the ratio of TUNEL-positive nuclei to the total number of cardiac cells within the field of view.

2.7. DHE

H9c2 cells (2 × 105) were seeded in 6-well plates with 2 mL of growth medium. Once the cells reached 60% confluence, they were treated with 140 μM ISO for 48 hours. The culture medium was then replaced with a fresh medium containing 10% FBS. For reactive oxygen species (ROS) detection, the cells were incubated with 25 μM DHE (Beyotime, S0063) for 25 minutes at 37 °C in the dark. Following incubation, the DHE-containing medium was discarded, and the wells were rinsed with 0.01 M PBS. Intracellular oxidative stress was assessed via fluorescence microscopy, and data were acquired using a FACS flow cytometer. FlowJo V10 software was used to perform quantitative analysis of free radicals. Cell populations were gated based on size and granularity (SSC-A vs. FCS-A), and the fluorescence intensity of the gated cells was analyzed to evaluate the antioxidant capacity of the enzymes. The control group served as the negative reference, while the ISO-treated group was the positive control.

 doi:10.20944/preprints202504.0915.v1

2.8. LDH Assay

Supernatants from the cell culture were collected, and lactate dehydrogenase (LDH) release was assessed to determine cellular damage, following the kit's protocol. Absorbance was measured at 450 nm.

2.9. Cell Viability Assay

Cells were exposed to varying concentrations (0, 40, 80, 100, 120, 140, 160, or 180 μM) of ISO in the culture medium for 24, 48, or 72 hours. After incubation, the medium was replaced with a fresh medium containing CCK-8 reagent (APExBio). Following an additional 2–3 hour incubation, absorbance was measured at 450 nm using a Thermo Fisher microplate reader. Cell viability was determined by comparing the absorbance values to those of untreated control cells.

2.10. Flow Cytometry Assay_Annexin-V/PI Assay for Apoptosis

Apoptosis was assessed using the Annexin V-FITC/PI Apoptosis Detection Kit. Cells were incubated with 5 μL of Annexin V-FITC and 10 μL of PI solution, then analyzed by flow cytometry. The percentage of apoptotic cells was calculated using FlowJo V10 software.

2.11. Western Blot Analysis

Proteins were extracted from cardiac tissue or cells using RIPA lysis buffer, and protein concentration was quantified via the BCA assay kit. Proteins were separated by 10% SDS-PAGE and transferred onto PVDF membranes. Membranes were blocked with 5% non-fat milk for 2 hours at room temperature, then incubated with primary antibodies overnight at 4 °C. Afterward, membranes were incubated with horseradish peroxidase-conjugated secondary antibodies (diluted 1:20,000) for 2 hours. Chemiluminescent signals were detected using an ECL kit and captured via a chemiluminescence imaging system. Images were saved for further quantitative analysis, with β-actin as the internal control.

2.12. Gene Set Enrichment Analysis (GSEA)

H9c2 cells were grouped into control, ISO, and ISO + Isor treatment conditions. RNA was extracted from H9c2 cells using TRIzol reagent, and the samples were sent to NovelBio (Shanghai, China) for further analysis.

2.13. RNA Extraction and RNA Sequencing Analysis

Transcriptomic data were processed using the OmicShare platform (https://www.omicshare.com/), utilizing the dynamic GSEA enrichment tool, selecting "Homo sapiens (GRCh38.p13)" for species. The Molecular Signature Database (MSigDB) was employed to identify hallmark gene sets, facilitating the identification of key targets and mechanisms through which isorhamnetin modulates ISO-induced myocardial injury, based on the expression profiles of differentially expressed genes (DEGs).

2.14. Docking Analysis

The molecular docking study was conducted using AutoDockTools 1.5.7 to investigate the binding interactions between isorhamnetin and its primary target. The 3D structure of isorhamnetin was retrieved from the PubChem database (https://pubchem.ncbi.nlm.nih.gov/), and the structure of the primary target protein was obtained from the PDB database (https://www.rcsb.org/). The target protein's structure was refined using PyMol. Isorhamnetin was set as a ligand for semiflexible docking with the target, using AutoDockTools. Binding interactions and modes were analyzed, and the configurations with the lowest binding energies were visualized.

 doi:10.20944/preprints202504.0915.v1

2.15. RNA Knockdown

The ENO1-targeted small interfering RNA (siRNA) was purchased from JTS Scientific, Wuhan, China. A non-specific siRNA was used as the negative control. Cells were transfected with the siRNA using a reagent provided by Gene Pharma (China) and cultured for 48 hours according to the manufacturer's protocol. Transfection efficacy was assessed using Western blot analysis. The specific sequence for ENO1 was 5'-GAGCAGAGGUUUACCACAATT-3', and the complementary sequence was 3'-UUGUGGUAAACCUCUGCUCTT-5'.

2.16. Statistical Analysis

The experimental data were analyzed using GraphPad Prism 9.0, and differences between groups were assessed using one-way ANOVA. Results are expressed as mean ± standard deviation (S.D.), with visual charts generated for clarity. Statistical significance was defined as $p < 0.05$. Specifically, $^{*}p < 0.05$, $^{**}p < 0.01$, $^{***}p < 0.001$ compared to the control group, and $\#p < 0.05$, $\#\#p < 0.01$, $\#\#\#p < 0.001$ compared to the ISO group.

3. Results

3.1. Isorhamnetin Ameliorates ISO-Induced Cardiac Dysfunction in a Rat Model

3.1.1. Evaluating Cardiac Function via Echocardiography

Echocardiography was employed to evaluate cardiac function in rats. As shown in Figure 1A, rats administered isoprenaline via intraperitoneal injection exhibited significant cardiac dysfunction compared to the control group. However, treatment with isorhamnetin and the positive control, propranolol, notably improved cardiac performance. Left ventricular ejection fraction (EF%) and fractional shortening (FS%) values, measured by echocardiography, are presented in Figure 1B. EF% and FS% in the ISO model group were significantly lower than in the control group, whereas those in the isorhamnetin and propranolol pre-treated groups were considerably elevated. These results indicate that isorhamnetin alleviates ISO-induced cardiac damage. Furthermore, the enhancement of EF% and FS% by isorhamnetin was dose-dependent, with its protective effect paralleling that of the positive control drug, propranolol.

3.1.2. Isorhamnetin Alleviates ISO-Induced Myocardial Histopathological Damage and Myocardial Fibrosis in Rats

The pathological histological changes in cardiac tissue across groups were assessed using HE staining. As illustrated in Figure 1C, both isorhamnetin and the positive control, propranolol, mitigated ISO-induced pathological alterations in the heart. In normal cardiac tissue, myocardial cells displayed a uniform shape with distinct longitudinal and transverse striations, and myofibrils were neatly organized. In contrast, the ISO model group exhibited varying degrees of cell swelling, vacuolar degeneration, cytoplasmic coagulation, dense nuclei, disordered myocardial fibers, inflammatory cell infiltration, and occasional hemorrhage. Treatment with isorhamnetin and propranolol led to substantial improvements in myofiber alignment and reduced interstitial edema, with the high-dose isorhamnetin group showing a cellular structure closely resembling that of the normal group. To assess fibrous tissue formation, Masson staining was performed. The ISO group displayed marked fibrosis compared to the control, whereas myocardial fibrosis was progressively reduced in the isorhamnetin and propranolol treatment groups. These results suggest that isorhamnetin effectively prevents ISO-induced myocardial fibrosis. As shown in Figure 1E, serum levels of CK-MB and cTnI were significantly elevated in the ISO model group, indicating myocardial damage. However, these markers were markedly reduced in the ISO + Isor-5 mg/kg, ISO + Isor-10 mg/kg, and ISO + Pro-10 mg/kg pretreatment groups, demonstrating a dose-dependent attenuation

 doi:10.20944/preprints202504.0915.v1

of myocardial injury. These results indicate that isorhamnetin significantly alleviates ISO-induced myocardial injury in rats.

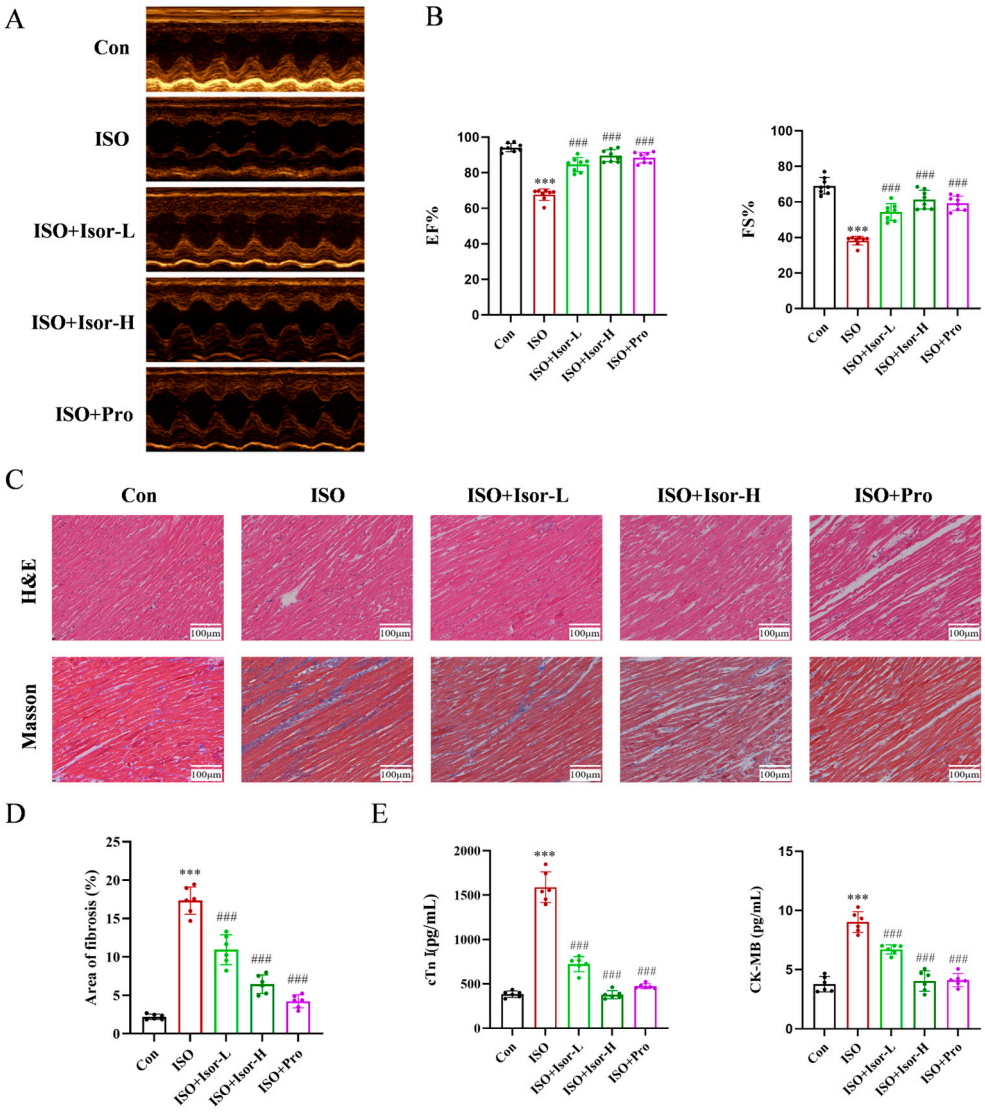

Figure 1. Effects of isorhamnetin on cardiac function indices. (A) M-mode echocardiograms of different groups. (B) Echocardiographic assessment of EF% and FS% for quantification of impaired cardiac function, n = 8. (C) Representative H&E and Masson's trichrome-stained images of rat myocardial tissue from each group (scale bar = 100 μm). (D) Statistical analysis of the fibrosis area in myocardial tissue across groups, n = 6. (E) Effect of isorhamnetin on the enzyme activities of cTnI and CK-MB in ISO-treated rats, n = 6. Data are expressed as means ± SDs. ***$p < 0.001$ vs. the control group; ###$p < 0.001$ vs. the ISO group.

3.2. Isorhamnetin Reduces ISO-Induced Apoptosis and Oxidative Stress in Rats

3.2.1. Isorhamnetin Alleviates ISO-Induced Myocardial Apoptosis in Rats

TUNEL fluorescence staining was employed to assess myocardial cell apoptosis. As shown in Figure 2A, the ISO model group exhibited a significantly higher number of apoptotic cardiomyocytes compared to the control group. In contrast, both the high-dose isorhamnetin and propranolol pretreatment groups demonstrated a marked reduction in apoptotic cardiomyocyte count relative to the model group. Immunoblotting data presented in Figure 2C revealed that, compared to the control

 doi:10.20944/preprints202504.0915.v1

group, the ISO model group showed a significant decrease in the anti-apoptotic protein Bcl-2, accompanied by an increase in the pro-apoptotic proteins Bax and cleaved caspase-3. Treatment with isorhamnetin and propranolol led to a substantial reduction in Bax and cleaved caspase-3 levels, along with an elevation in Bcl-2 expression. Notably, higher concentrations of isorhamnetin exerted a more pronounced effect on apoptosis-related proteins than the positive control, propranolol.

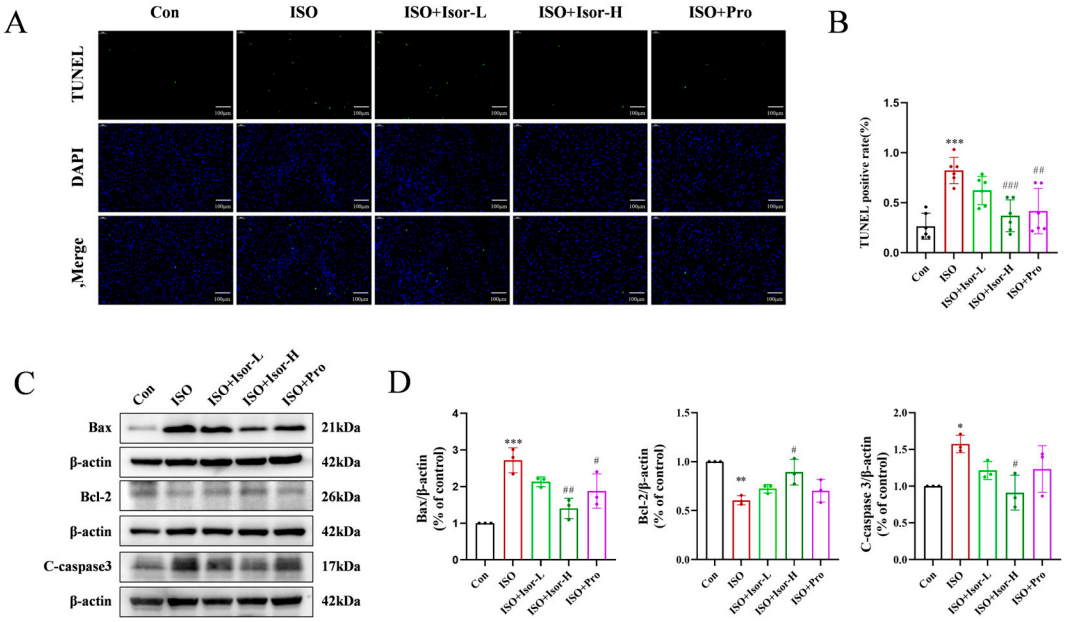

Figure 2. Isorhamnetin ameliorates ISO-induced myocardial apoptosis in rats. Schemes follow the same formatting. (A) Effect of isorhamnetin on ISO-induced myocardial apoptosis, as shown by TUNEL staining. (B) Statistical analysis of TUNEL assay results for each group, $n = 6$. (C, D) Effects of isorhamnetin on ISO-induced expression of Bcl-2, Bax, and cleaved caspase-3 proteins in the rat myocardium, $n = 3$. Data are expressed as means ± SDs. *$p < 0.05$, **$p < 0.01$, ***$p < 0.001$ vs. the control group; #$p < 0.05$, ##$p < 0.01$, ###$p < 0.001$ vs. the ISO group.

3.2.2. Isorhamnetin Alleviates ISO-Induced Myocardial Oxidative Stress in Rats

ROS levels in the cardiac tissue of rats were assessed using DHE staining. As shown in Figure 3A, the myocardium of the ISO model group exhibited more intense and widespread red fluorescence compared to the control group, indicating elevated ROS levels and substantial oxidative stress. In contrast, ROS levels were significantly reduced in the hearts of the ISO + Isor-5 mg/kg, ISO + Isor-10 mg/kg, and ISO + Pro-10 mg/kg groups, suggesting that isorhamnetin effectively mitigates oxidative stress in rat hearts.

The expression of oxidative stress-related proteins Nrf2, HO-1, and NQO1 was evaluated in rat heart tissues through immunoblotting. As shown in Figure 3C, these proteins were detectable in the cardiac tissues. Compared to the control group, the ISO model group exhibited a significant reduction in the expression of Nrf2, HO-1, and NQO1. In contrast, pretreatment with high doses of isorhamnetin and propranolol resulted in a marked increase in HO-1 and NQO1 expression in the heart tissues.

To assess systemic oxidative stress, serum levels of GSH-PX, SOD, and MDA were measured. As shown in Figure 3E, the ISO group exhibited significantly reduced SOD and GSH-PX activities and elevated MDA levels compared to the control group, indicating increased oxidative stress following ISO administration. In contrast, the ISO + Isor-5 mg/kg, ISO + Isor-10 mg/kg, and ISO + Pro-10 mg/kg groups displayed significantly lower MDA levels and notably higher SOD and GSH-PX

 doi:10.20944/preprints202504.0915.v1

activities compared to the ISO group. These results demonstrate that isorhamnetin effectively alleviates ISO-induced myocardial oxidative stress in rats.

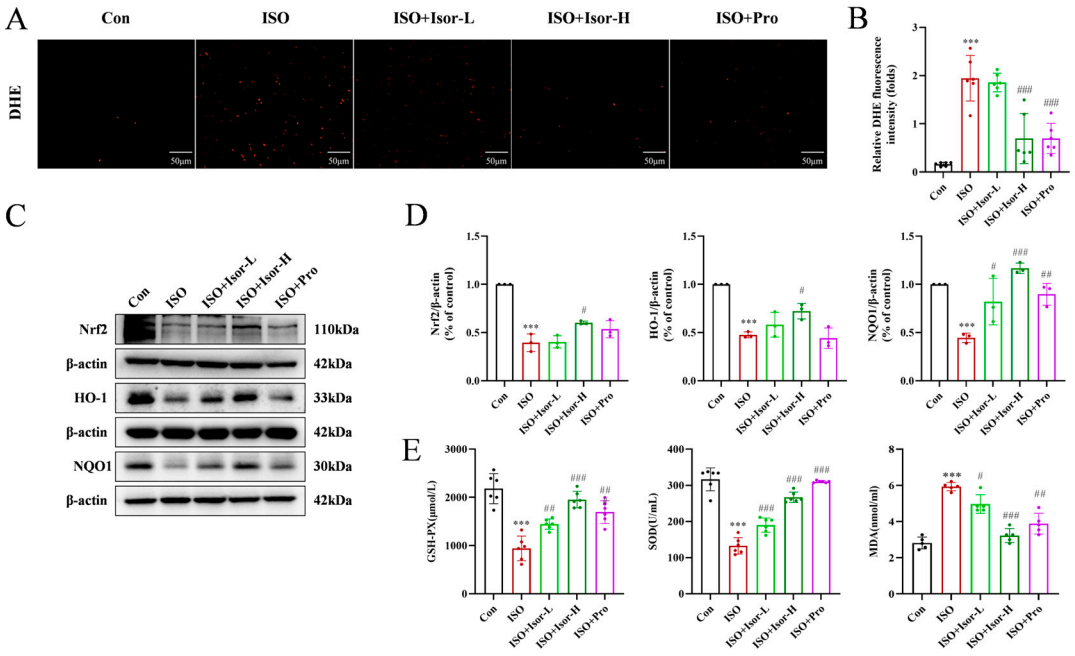

Figure 3. Isorhamnetin ameliorates ISO-induced oxidative stress in the rat myocardium. (A, B) Effects of isorhamnetin on ISO-induced myocardial oxidative stress in rats, as shown by DHE staining, $n = 6$. (C, D) Effects of isorhamnetin on ISO-induced Nrf2, HO-1, and NQO1 protein expression in the rat myocardium, $n = 3$. (E) Effects of isorhamnetin on the activities of GSH-PX, SOD, and MDA enzymes in ISO-treated rats, $n = 6$. Data are expressed as means ± SDs. ***$p < 0.001$ vs. the control group; #$p < 0.05$, ##$p < 0.01$, ###$p < 0.001$ vs. the ISO group.

3.3. Isorhamnetin Increases Cell Viability and Alleviates Myocardial Injury in ISO-Injured H9c2 Cells

The CCK-8 assay was employed to assess the viability of H9c2 cells, enabling the determination of optimal concentrations for ISO and isorhamnetin, as well as the exposure duration. As shown in Figure 4A, after 48 hours of exposure to ISO at concentrations ranging from 0 to 200 μM, cell viability increased with ISO concentration up to 80 μM. However, higher ISO concentrations resulted in reduced cell viability, with a significant decrease observed at 140 μM, establishing this concentration as the threshold for inducing cellular damage in subsequent experiments.

To evaluate the potential toxicity of isorhamnetin on H9c2 cells, various concentrations (0, 0.3125, 0.625, 1.25, 2.5, and 5 μM) were tested using the CCK-8 assay. Figure 4B demonstrates that isorhamnetin concentrations up to 5 μM did not significantly affect cell survival after 48 hours, suggesting its non-toxic nature at these concentrations. Based on these results, concentrations of 0.625, 1.25, and 2.5 μM were selected for pretreatment. Cells were pretreated with these concentrations of isorhamnetin, followed by 140 μM ISO treatment for 48 hours, as shown in Figure 4C. The results indicate that isorhamnetin effectively mitigates the reduction in cell viability caused by ISO. Additionally, the LDH assay results (Figure 4D) reveal a significant increase in intracellular LDH levels after ISO treatment, reflecting myocardial cell damage. In contrast, the LDH levels in the isorhamnetin-treated groups, at low, medium, and high concentrations, were progressively lower than those in the ISO model group, suggesting that isorhamnetin provides protective effects against ISO-induced cardiomyocyte injury.

 doi:10.20944/preprints202504.0915.v1

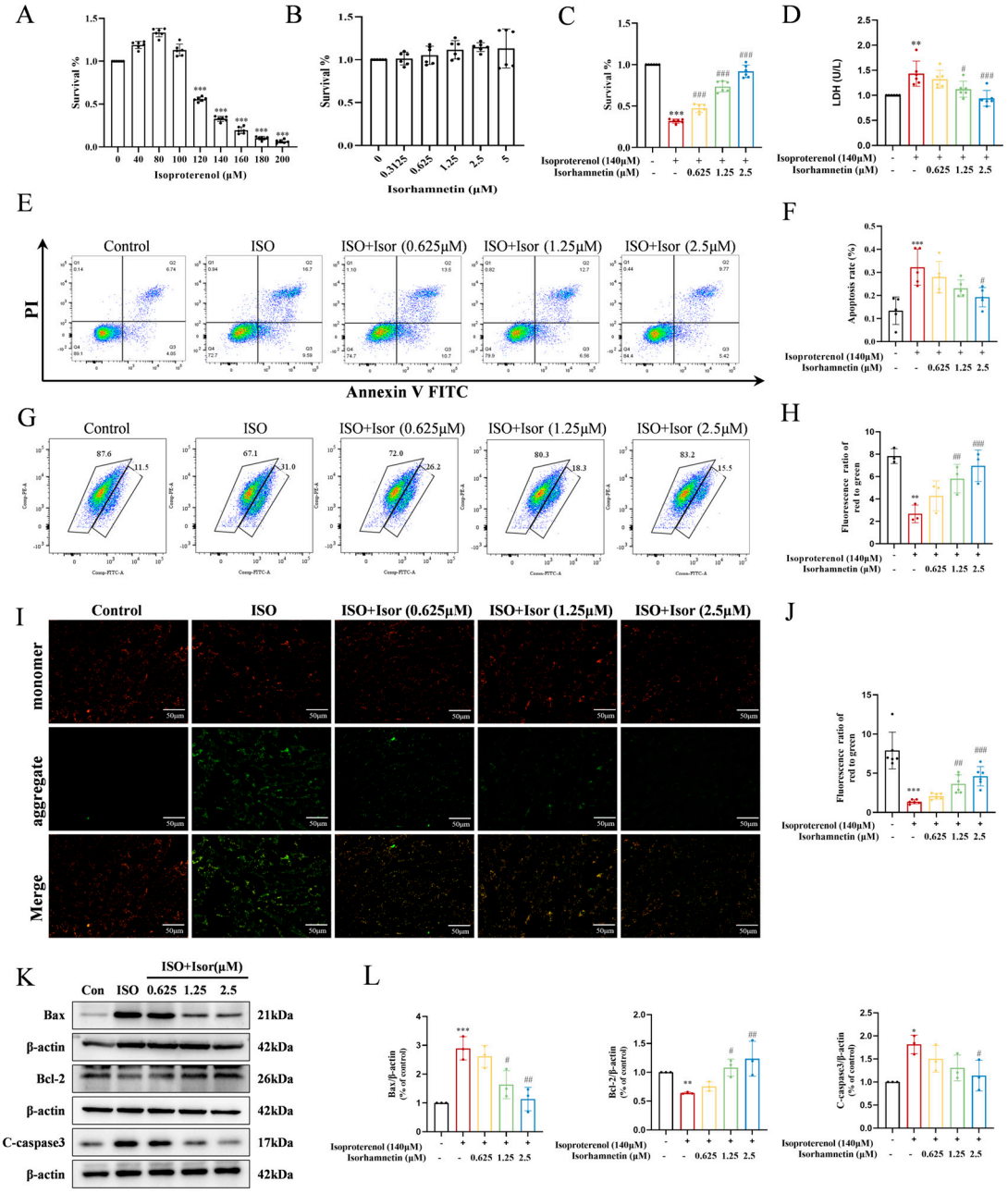

Figure 4. Isorhamnetin ameliorates ISO-induced H9c2 cardiomyocyte injury. (A) Effect of ISO on the survival rate of H9c2 cardiomyocytes, $n = 6$. (B) Effects of different concentrations of isorhamnetin on the survival rate of H9c2 cells, $n = 6$. (C) Effect of isorhamnetin on the survival rate of ISO-treated H9c2 cells, $n = 6$. (D) Effect of isorhamnetin on LDH activity in ISO-treated H9c2 cells, $n = 6$. (E, F) Effects of isorhamnetin on ISO-induced apoptosis in H9c2 cells, assessed by flow cytometry, $n = 5$. (G, H) JC-1 staining combined with flow cytometry analysis, $n = 3$. (I, J) JC-1 staining observed under an inverted microscope, $n = 6$. (K, L) Effects of isorhamnetin on ISO-induced protein expression of Bax, Bcl-2, and cleaved caspase-3 in H9c2 cells, as detected by Western blotting, $n = 3$. Data are expressed as means ± SDs. $^{*}p < 0.05$, $^{**}p < 0.01$, $^{***}p < 0.001$ vs. the control group; $\#p < 0.05$, $\#\#p < 0.01$, $\#\#\#p < 0.001$ vs. the ISO group.

 doi:10.20944/preprints202504.0915.v1

3.4. Isorhamnetin Reduces ISO-Induced Apoptosis and Oxidative Stress In Vitro

3.4.1. Isorhamnetin Alleviates ISO-Induced Myocardial Oxidative Stress in Rats

Apoptosis in H9c2 cardiomyocytes was evaluated via Annexin V-FITC/PI dual-staining and flow cytometry. As depicted in Figure 4E, the model group exhibited a markedly higher apoptotic cell count in the Q2+Q3 region compared to the control group. In contrast, the high-dose isorhamnetin-pretreated group showed a significantly lower percentage of apoptotic cells, suggesting that isorhamnetin mitigates ISO-induced cardiomyocyte apoptosis. The underlying mechanism of ISO-induced apoptosis was further investigated using JC-1 staining and flow cytometry, with results shown in Figure 4G-J. ISO treatment notably reduced mitochondrial membrane potential in H9c2 cells relative to controls, whereas pre-treatment with 0.625, 1.25, and 2.5 μM isorhamnetin restored mitochondrial membrane potential in a concentration-dependent manner. To assess the impact of isorhamnetin on apoptosis, the expression of key apoptosis-related proteins—Bax, cleaved caspase-3, and Bcl-2—was examined through immunoblotting. In comparison to controls, the ISO group displayed significantly elevated levels of the pro-apoptotic proteins Bax and cleaved caspase-3, alongside a decrease in the anti-apoptotic protein Bcl-2. Pre-treatment with isorhamnetin, particularly at 2.5 μM, led to a notable reduction in Bax and cleaved caspase-3 levels, while enhancing Bcl-2 expression. These results confirm that isorhamnetin effectively attenuates ISO-induced cardiomyocyte apoptosis.

3.4.2. Isorhamnetin Reduces ISO-Induced Oxidative Stress In Vitro

As illustrated in Figure 5A, DHE fluorescence was utilized to assess the impact of isorhamnetin on ROS levels in ISO-treated H9c2 cardiomyocytes. The model group exhibited a significantly higher number of cells with red fluorescence compared to the control group. However, pretreatment with isorhamnetin at concentrations of 0.625, 1.25, and 2.5 μM led to a dose-dependent reduction in the number of cells showing red fluorescence, relative to the ISO group. The fluorescence intensity in the ISO group was markedly elevated compared to the control group, indicating a significant increase in ROS levels in H9c2 cardiomyocytes. In contrast, the fluorescence intensity in cells pretreated with various concentrations of isorhamnetin progressively decreased, reflecting a reduction in ROS content, with the effect becoming more pronounced at higher concentrations of isorhamnetin (Figure 5C). As shown in Figure 5E, the expression of Nrf2, HO-1, and NQO1 was lower in the ISO group compared to controls. In contrast, isorhamnetin pretreatment induced a concentration-dependent increase in the expression of these antioxidant markers, relative to the model group. These results suggest that isorhamnetin effectively mitigates ISO-induced oxidative stress in H9c2 cells.

 doi:10.20944/preprints202504.0915.v1

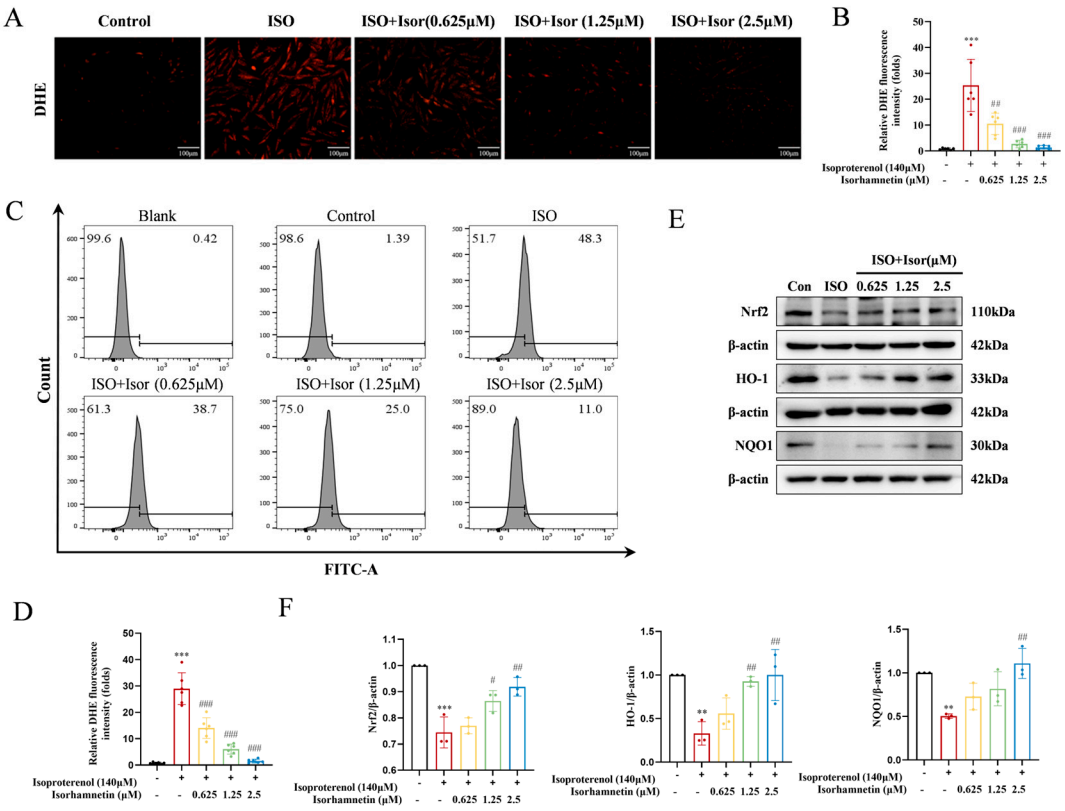

Figure 5. Isorhamnetin attenuates ISO-induced oxidative stress in H9c2 cells. (A, B) DHE fluorescence in each group, $n = 6$. (C, D) DHE combined with flow cytometry data, $n = 6$. (E, F) Effects of isorhamnetin on the ISO-induced protein expression of Nrf2, HO-1, and NQO1 in H9c2 cells, as detected by Western blotting, $n = 3$. Data are expressed as means ± SDs. $^{**}p < 0.01$, $^{***}p < 0.001$ vs. the control group; $^{\#}p < 0.05$, $^{\#\#}p < 0.01$, $^{\#\#\#}p < 0.001$ vs. the ISO group.

3.5. Transcriptome Sequencing Enrichment Reveals the Inhibition of the Glycolytic Pathway After Isorhamnetin Treatment, with ENO1 as a Key Target

To investigate the regulatory effects of isorhamnetin on ISO-induced injury in H9c2 cardiomyocytes, high-throughput transcriptomic sequencing was performed to analyze gene expression profiles in control, ISO, and ISO+Isor (1.25 μM) groups. The analysis identified 7560 DEGs compared to the control group. Following isorhamnetin pretreatment, 11 genes were downregulated and 12 upregulated relative to the ISO group. Figure 6A displays a heatmap of DEGs post-isorhamnetin treatment, with green indicating downregulation and red representing upregulation. GO enrichment analysis emphasized the role of the negative regulation of cysteine-type endopeptidases in apoptosis (Figure 6B), while KEGG pathway analysis highlighted the significance of the PPAR pathway (Figure 6C). GSEA of the DEGs revealed significant suppression of the glycolytic gene set, with an enrichment score (ES) of -0.6463721 and a false discovery rate (FDR) of 0.001 (Figure 6D). The gene expression clustering plot for glycolytic metabolism showed that ENO1 was significantly downregulated, with a Log2FC of -0.676 and an FDR of 0 (corrected $p < 0.001$), suggesting ENO1's pivotal role in glycolytic metabolism after isorhamnetin treatment. Molecular docking simulations were carried out to assess the interaction between isorhamnetin and ENO1, PPARα, and PGC-1α, with binding stability determined by docking scores. Figures 6F-H illustrate the binding patterns of isorhamnetin with ENO1, PPARα, and PGC-1α, showing binding energies below -1.2 kcal/mol, indicating robust binding. The lowest binding energies for isorhamnetin with ENO1, PPARα, and PGC-1α were -4.54, -7.16, and -8.05 kcal/mol, respectively, confirming isorhamnetin's strong binding affinity for these molecules.

 doi:10.20944/preprints202504.0915.v1

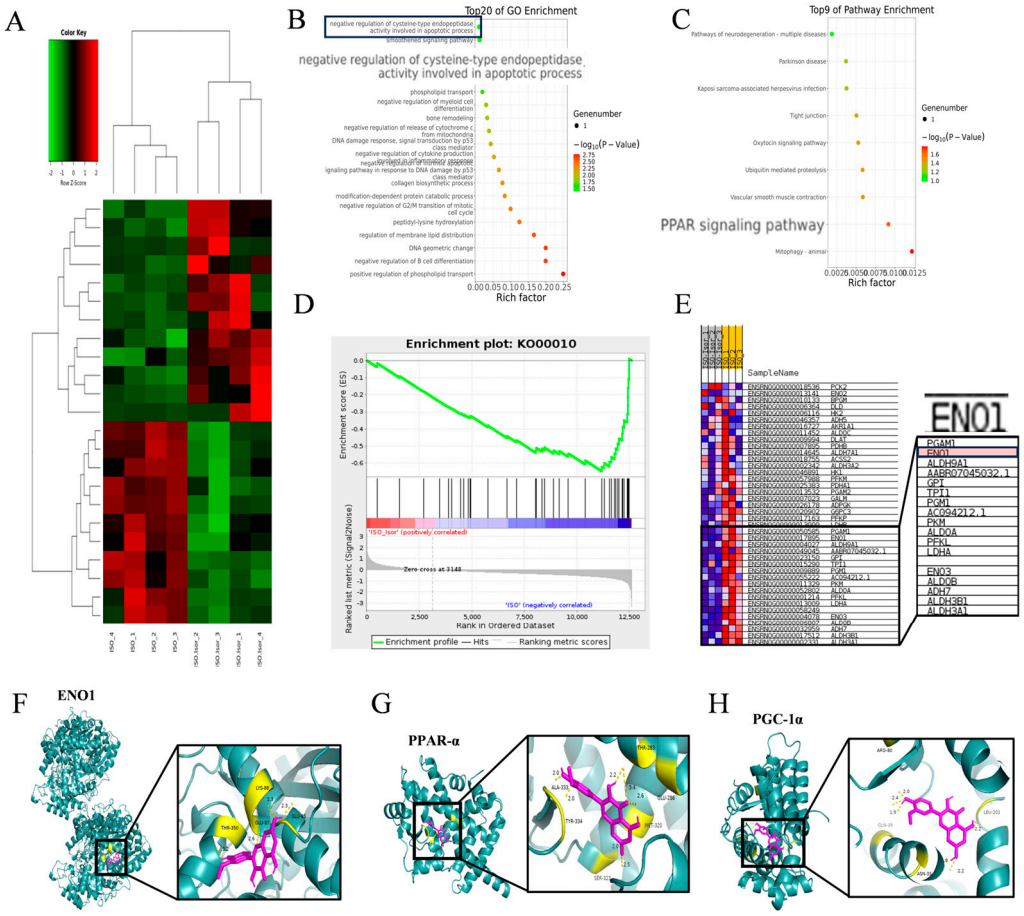

Figure 6. Transcriptome sequencing revealed inhibition of the glycolytic pathway after isorhamnetin treatment, with ENO1 as a key target. (A) RNA sequencing results showing differential gene expression in ISO-induced H9c2 cardiomyocytes treated with isorhamnetin. (B, C) Z-score bubble chart of KEGG and GO enrichment analyses of the DEGs identified via transcriptomics (upward normalization). (D) GSEA enrichment plot for the glycolytic metabolism gene set. (E) Gene expression clustering plot for the glycolytic metabolism gene set. (F-H) Molecular docking patterns of isorhamnetin with ENO1, PPARα, and PGC-1α molecules.

3.6. Transcriptome Sequencing Enrichment Reveals the Inhibition of the Glycolytic Pathway After Isorhamnetin Treatment, with ENO1 as a Key Target

Transcriptomic analysis highlighted the pivotal role of the glycolytic pathway in ISO-induced cardiac injury. Significant alterations in glucose, the primary substrate for glycolysis, and lactate, its end product, were observed (Figure 7A and B). The ISO model group exhibited markedly higher levels of intracellular glucose and lactate compared to the control group. These levels were progressively reduced with increasing isorhamnetin concentrations, suggesting that ISO treatment enhances glycolysis, while isorhamnetin inhibits this process. Regarding energy metabolism, glycolytically-derived ATP levels were notably lower than those generated via fatty acid metabolism. As shown in Figure 7C, ATP levels in the ISO-treated group were significantly reduced compared to controls, and isorhamnetin mitigated the ISO-induced decrease in cytoplasmic ATP content. To further investigate, immunoblotting was performed to assess the expression of ENO1, a key glycolytic enzyme, as well as PPARα and PGC-1α, key regulators in the PPAR signaling pathway, in H9c2 cells across control, ISO, and ISO+Isor (1.25 μM) groups. Figure 7D illustrates that ISO treatment led to a significant upregulation of ENO1 and downregulation of PPARα and PGC-1α expression. In contrast, isorhamnetin pretreatment reversed these changes, reducing ENO1 expression while

 doi:10.20944/preprints202504.0915.v1

enhancing PPARα and PGC-1α levels. These results indicate that isorhamnetin effectively counteracts ISO-induced glycolysis and exerts a protective effect on cardiac function.

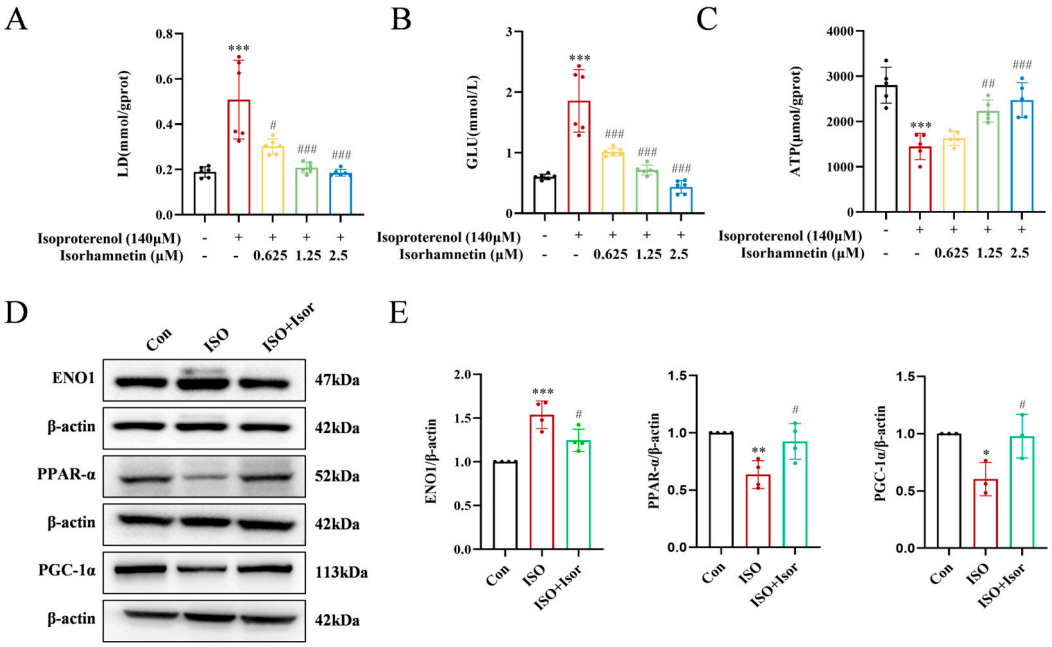

Figure 7. Isorhamnetin reversed the ISO-induced increase in intracellular glycolytic processes and increased ATP content. (A-C) Statistical graphs showing lactate, glucose, and ATP contents, $n = 5, 6$. (D, E) Immunoblotting bands displaying the protein expression of ENO1, PPAR-α, and PGC-1α in cells, $n = 3, 4$. Data are expressed as means ± SDs. *$p < 0.05$, **$p < 0.01$, ***$p < 0.001$ vs. the control group; #$p < 0.05$, ##$p < 0.01$, ###$p < 0.001$ vs. the ISO group.

3.7. Isorhamnetin Exerts Cardioprotective Effects by Inhibiting ENO1, Activating the PPARα/PGC-1α Signaling Axis, Reversing Isoprenaline-Induced Conversion of H9c2 Energy Metabolism Substrate Levels, Inhibiting Glycolysis, and Increasing ATP Release, Thereby Attenuating Apoptosis and Oxidative Stress

To investigate the cardioprotective potential of isorhamnetin, ENO1 inhibition was employed using AP-III-a4, a non-substrate analog that binds to enolase and inhibits its activity in H9c2 cells. Glucose, the primary glycolytic substrate, and lactate, a glycolytic byproduct, were measured as shown in Figure 8A and B. The ISO model group exhibited significantly elevated intracellular glucose and lactate levels compared to the control group. In contrast, the AP-III-a4 inhibitor group displayed markedly reduced glucose and lactate levels, mirroring the protective effects of isorhamnetin. The combined treatment of AP-III-a4 and isorhamnetin further decreased these levels. As illustrated in Figure 8C, intracellular ATP content was significantly reduced in the ISO-treated group compared to controls. AP-III-a4 treatment mitigated the ISO-induced decline in ATP, and the ATP level was notably increased when both AP-III-a4 and isorhamnetin were used in combination.

To further explore the role of ENO1 in myocardial damage, siRNA targeting ENO1 was introduced into H9c2 cells, and knockdown efficiency was confirmed by Western blot analysis. The expression of apoptosis and oxidative stress markers was also assessed. The results showed that silencing ENO1 in H9c2 cells produced effects similar to isorhamnetin treatment. Specifically, ENO1 suppression reduced the expression of pro-apoptotic markers Bax and cleaved caspase-3, while enhancing the anti-apoptotic protein Bcl-2. Additionally, increased expression of oxidative stress-related markers, including Nrf2, HO-1, and NQO1, was observed (Figure 8D, E). These results collectively highlight the critical role of ENO1 in mediating cardiomyocyte injury.

 doi:10.20944/preprints202504.0915.v1

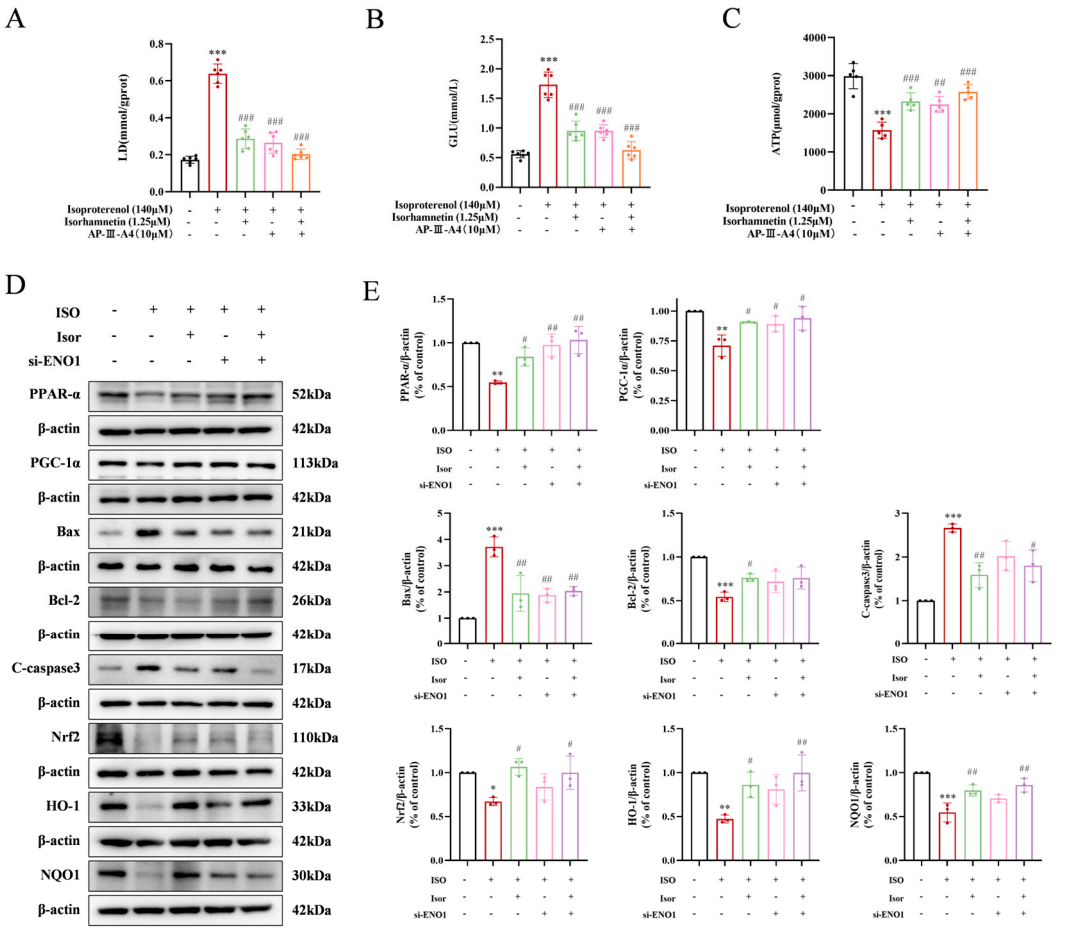

Figure 8. Isorhamnetin inhibits ENO1, activates the PPARα/PGC-1α signaling axis, reverses the transformation of H9c2 energy metabolism substrates induced by isoproterenol, inhibits glycolysis, increases ATP release, alleviates apoptosis and oxidative stress, and protects against cardiac injury. (A-C) Statistical graphs showing lactate, glucose, and ATP contents, $n = 5, 6$. (D-E) Western blot analysis of apoptosis, oxidative stress, and PPAR signaling pathway-related protein expression; β-actin was used as a control, $n = 3$. Data are expressed as means ± SDs. $^{*}p < 0.05$, $^{**}p < 0.01$, $^{***}p < 0.001$ vs. the control group; $^{\#}p < 0.05$, $^{\#\#}p < 0.01$, $^{\#\#\#}p < 0.001$ vs. the ISO group.

 doi:10.20944/preprints202504.0915.v1

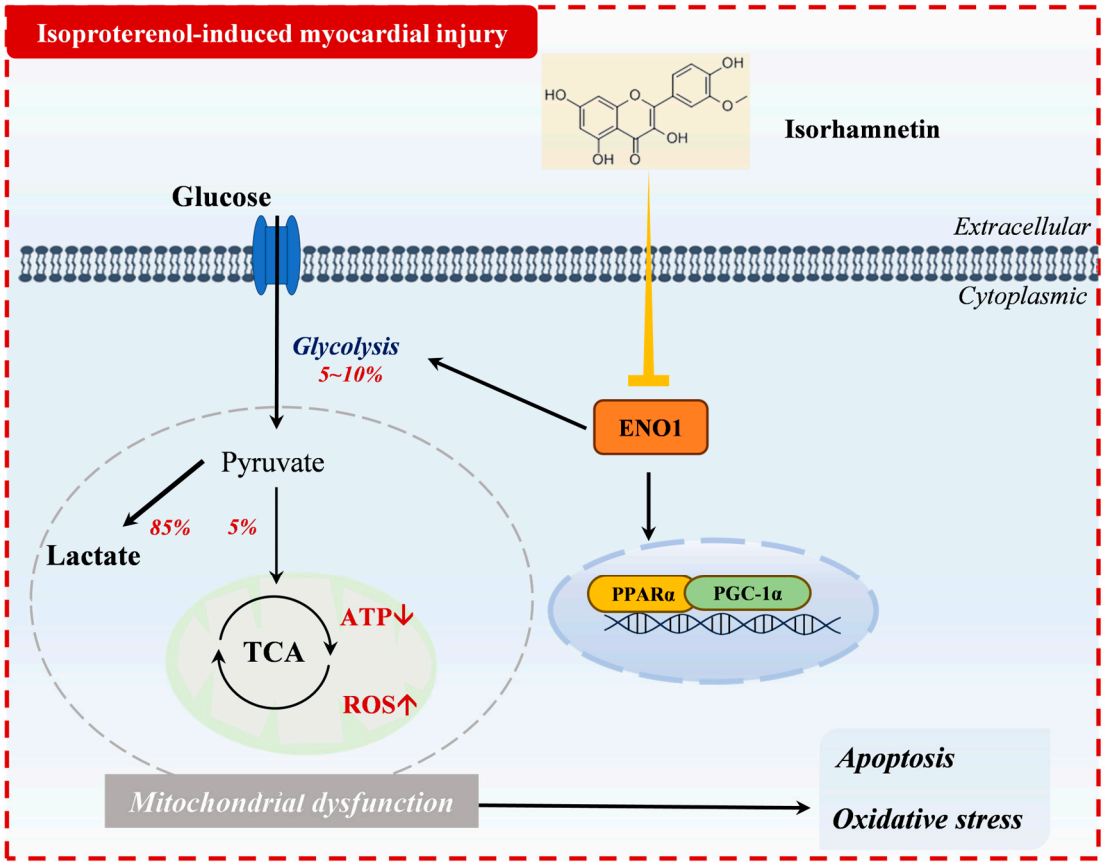

Figure 9. Mechanism of action of isorhamnetin in isoprenaline-induced myocardial injury.

4. Discussion

ISO, a β-adrenergic receptor agonist, plays a pivotal role in clinical conditions such as myocardial infarction, arrhythmia, heart failure, and stress-related heart diseases [8,20]. Currently, propranolol is the primary treatment for these conditions, but it is associated with adverse effects, including central nervous system disturbances, bronchospasm, and congestive heart failure [21,22]. Thus, identifying more effective therapeutic strategies and novel targets for intervention is essential. Isorhamnetin, a natural flavonoid [23], has garnered attention due to its diverse biological activities. Recent studies highlight its potential as an anti-apoptotic, antioxidant, and anti-inflammatory agent, positioning it as a promising candidate for cardiovascular disease therapy [24]. For example, Xu et al. demonstrated that isorhamnetin could ameliorate myocardial apoptosis and oxidative stress induced by ischemia-reperfusion in SD rats [25]. These findings suggest that isorhamnetin may offer protective benefits against ISO-induced myocardial injury, prompting further experimental investigation into this hypothesis.

Apoptosis is a regulated form of cell death that facilitates the efficient removal of damaged cells, such as those caused by DNA damage or developmental processes [26]. Endogenous apoptosis is primarily governed by mitochondrial function [27,28]. Previous studies have indicated that inhibition of Bax activity and promotion of Bcl-2 expression could confer direct cardioprotection in acute myocardial infarction [18,29,30]. In the present study, isorhamnetin inhibited Bax expression, promoted Bcl-2 expression, and reduced Caspase-3 activation, thereby exerting an anti-apoptotic effect.

Increased oxidative stress is recognized as a common contributor to cardiovascular diseases [31]. Maintaining a delicate balance between ROS and antioxidants is essential for cellular function. Excessive ROS can damage cellular macromolecules such as DNA, lipids, and proteins, ultimately leading to necrosis and apoptosis [32,33]. In both animal and cellular models, DHE staining confirmed that isorhamnetin reduced ROS production induced by isoprenaline. Our experiments

 doi:10.20944/preprints202504.0915.v1

showed that, compared to the control group, the serum MDA levels were significantly elevated, while the levels of SOD and GSH-PX were reduced in the model group. These results align with findings from other studies [34–36]. Both isorhamnetin and propranolol were able to reverse these changes [37,38]. Nrf2 plays a pivotal role in mitigating oxidative stress, with HO-1 serving as a key mediator in reducing myocardial oxidative stress injury. Nrf2 activates the antioxidant response by translocating to the nucleus, where it binds to the promoter region of downstream genes, including HO-1 [39]. In the present study, both animal and cellular experiments demonstrated that isorhamnetin increased the expression of Nrf2, HO-1, and NQO1 in damaged cardiomyocytes, thereby enhancing the cellular antioxidant response. These results suggest that isorhamnetin may protect against ISO-induced oxidative stress damage. Furthermore, oxidative stress is intricately linked to mitochondrial dysfunction [40–42]. Mitochondria are central to heart failure pathophysiology, influencing processes such as energy metabolism, oxidative stress, calcium homeostasis, and cell death [43–45]. The JC-1 mitochondrial membrane potential assay revealed that isorhamnetin effectively reversed ISO-induced mitochondrial damage, indicating its cardioprotective effects.

To elucidate the mechanism via which isorhamnetin alleviates isoprenaline-induced myocardial injury, transcriptomic RNA sequencing was performed on H9c2 cells, ISO-treated H9c2 cells, and isorhamnetin-pretreated H9c2 cells. GSEA was conducted on all enriched genes. Compared to the ISO group, isorhamnetin pretreatment significantly reduced the expression of several glycolytic metabolism genes, with ENO1 identified as a key target for this downregulation. ENO1, a glycolytic enzyme involved in the ninth step of glycolysis, has been implicated in myocardial injury. Ji et al. demonstrated that serpina3c alleviates myocardial fibrosis post-MI by inhibiting ENO1 transcriptional activation, thereby suppressing glycolysis [11]. Wu et al. further reported that elevated ENO1 expression leads to myocardial apoptosis, impaired collagen deposition, and systolic dysfunction [9]. Molecular docking revealed a strong affinity between isorhamnetin and ENO1, suggesting ENO1 as a direct target of isorhamnetin. PPARs, a key class of nuclear hormone receptors, regulate numerous cellular functions, with isoforms PPARα, PPARβ, and PPARγ playing pivotal roles in physiological processes [46]. PPARα, predominantly expressed in the myocardium, is a critical transcription factor in myocardial energy metabolism remodeling [47]. Activation of peroxisome proliferator-activated receptor γ coactivator 1α (PGC-1α) enhances the transcription of genes encoding enzymes involved in myocardial energy metabolism, such as PGC-1α, through paracrine signaling [48]. The upregulation of PGC-1α boosts mitochondrial fatty acid metabolism, promoting oxidative FA metabolism and inhibiting glycolysis, thereby facilitating adenosine triphosphate (ATP) production and mitigating chronic heart failure [49]. Immunoblotting experiments demonstrated increased ENO1 protein expression, alongside decreased PPARα and PGC-1α protein levels, in rat heart tissues exposed to ISO. These results suggest that the protective effect of isorhamnetin may be linked to ENO1 and glycolytic metabolism. It is hypothesized that PPARα may regulate isorhamnetin-mediated ENO1 transcription, thereby modulating the myocardial response to isoprenaline-induced injury. Notably, during the onset of ISO-induced myocardial injury, key glycolytic enzymes were upregulated while ATP production decreased, indicating a metabolic shift from fatty acid metabolism to anaerobic glucose glycolysis [50]. This metabolic shift was reversed upon isorhamnetin pretreatment. To further confirm the role of ENO1, the enolase inhibitor AP-III-a4 (ENOblock) was applied, resulting in similar reductions in intracellular glucose and lactate levels and enhanced ATP production compared to isorhamnetin alone [44,51]. The combined use of both agents yielded more pronounced therapeutic effects, suggesting that isorhamnetin's inhibition of ENO1 effectively suppresses glycolysis and improves energy metabolism.

In summary, this study identified ENO1 as a key player in isoprenaline-induced myocardial injury, integrating transcriptomic analysis with in vitro and ex vivo cellular experiments. For the first time, it demonstrates that isorhamnetin confers cardiovascular protection through targeting ENO1. Moreover, this research presents a novel perspective on isoprenaline-induced myocardial injury,

 doi:10.20944/preprints202504.0915.v1

highlighting the involvement of glucose metabolism. The inhibition of glycolysis and the correction of energy metabolism disturbances may underlie the cardiovascular protective effects of isorhamnetin. This study advances targeted therapy for cardiovascular diseases, broadens the understanding of isorhamnetin's pharmacological targets, and provides a foundation for further exploration of its natural bioactive compounds.

5. Conclusions

Isorhamnetin exerts cardioprotective effects by inhibiting ENO1, activating the PPARα/PGC-1α signaling axis, reversing isoprenaline-induced conversion of H9c2 energy metabolism substrate levels, inhibiting glycolysis, and increasing ATP release, thereby attenuating apoptosis and oxidative stress.

Author Contributions: Conceptualization, Zhenli Guo and Xinzhi Li; methodology, Shizhong Liu, Xianghong Hou, Xin Zhou and Yan Wang; software, Xin Zhou, Yan Wang and Yi Rong; validation, Shizhong Liu, Xianghong Hou, Rui Yang and Yi Rong; formal analysis, Ketao Ma; data curation, Zhenli Guo and Xinzhi Li; writing—original draft preparation, Zhenli Guo; writing—review and editing, Zhenli Guo and Rui Yang; supervision, Xinzhi Li; project administration, Ketao Ma; funding acquisition, Ketao Ma. All authors have read and agreed to the published version of the manuscript.

Funding: This study was supported by grants from the National Natural Science Foundation of China (No. 82460088), the Guiding Project of Xinjiang Production and Construction Corps (Nos. 2023ZD030 and 2023ZD035), the Training Program of Tianshan Talents to Ketao Ma.

Institutional Review Board Statement: All animal experiments and procedures were approved by the Institutional Animal Care and Use Committee of Shihezi University, in compliance with the university's ethical guidelines for animal experimentation.

Informed Consent Statement: Not applicable.

Data Availability Statement: The data used in this study are confidential.

Acknowledgments: Acknowledgments are extended to the Key Laboratory of Xinjiang Endemic and Ethnic Diseases and the Departments of Physiology and Pathophysiology at Shihezi University School of Medicine for their support.

Conflicts of Interest: The authors declare no known competing financial interests or personal relationships that could have influenced the work reported in this paper.

Abbreviations

The following abbreviations are used in this manuscript:

ISO	Isoproterenol
ATP	Adenosine Triphosphate
ENO1	Recombinant Enolase 1
PPAR	Peroxisome Proliferator-Activated Receptor
PGC-1	Peroxisome Proliferator-Activated Receptor Gamma Coactivator 1
CVDs	Cardiovascular Diseases
EF	Ejection Fraction
FS	Fractional Shortening
CK-MB	Creatine Kinase-MB
DHE	Dihydroethidium
Nrf2	NF-E2-related factor 2
HO-1	Heme Oxygenase 1
NQO1	Recombinant NADH Dehydrogenase, Quinone 1
MDA	Malondialdehyde

 doi:10.20944/preprints202504.0915.v1

SOD	Superoxide Dismutase
GSH-PX	Glutathione peroxidase
CCK-8	Cell Counting Kit-8
GSEA	Gene Set Enrichment Analysis

References

1. Roth, G. A., Mensah, G. A., Johnson, C. O., Addolorato, G., Ammirati, E., Baddour, L. M., Barengo, N. C., Beaton, A. Z., Benjamin, E. J., Benziger, C. P., Bonny, A., Brauer, M., Brodmann, M., Cahill, T. J., Carapetis, J., Catapano, A. L., Chugh, S. S., Cooper, L. T., Coresh, J., Criqui, M., … GBD-NHLBI-JACC Global Burden of Cardiovascular Diseases Writing Group (2020). Global Burden of Cardiovascular Diseases and Risk Factors, 1990-2019: Update From the GBD 2019 Study. *Journal of the American College of Cardiology*, 76(25), 2982–3021.
2. Lindstrom, M., DeCleene, N., Dorsey, H., Fuster, V., Johnson, C. O., LeGrand, K. E., Mensah, G. A., Razo, C., Stark, B., Varieur Turco, J., & Roth, G. A. (2022). Global Burden of Cardiovascular Diseases and Risks Collaboration, 1990-2021. *Journal of the American College of Cardiology*, 80(25), 2372–2425.
3. Nichtova, Z., Novotova, M., Kralova, E., & Stankovicova, T. (2012). Morphological and functional characteristics of models of experimental myocardial injury induced by isoproterenol. *General physiology and biophysics*, 31(2), 141–151.
4. Mukherjee, D., Ghosh, A. K., Dutta, M., Mitra, E., Mallick, S., Saha, B., Reiter, R. J., & Bandyopadhyay, D. (2015). Mechanisms of isoproterenol-induced cardiac mitochondrial damage: protective actions of melatonin. *Journal of pineal research*, 58(3), 275–290.
5. Liao, M., Xie, Q., Zhao, Y., Yang, C., Lin, C., Wang, G., Liu, B., & Zhu, L. (2022). Main active components of Si-Miao-Yong-An decoction (SMYAD) attenuate autophagy and apoptosis via the PDE5A-AKT and TLR4-NOX4 pathways in isoproterenol (ISO)-induced heart failure models. *Pharmacological research*, 176, 106077.
6. Qian, J. F., Liang, S. Q., Wang, Q. Y., Xu, J. C., Luo, W., Huang, W. J., Wu, G. J., & Liang, G. (2024). Isoproterenol induces MD2 activation by β-AR-cAMP-PKA-ROS signalling axis in cardiomyocytes and macrophages drives inflammatory heart failure. *Acta pharmacologica Sinica*, 45(3), 531–544.
7. van der Pol, A., van Gilst, W. H., Voors, A. A., & van der Meer, P. (2019). Treating oxidative stress in heart failure: past, present and future. *European journal of heart failure*, 21(4), 425–435.
8. Li, P., Luo, S., Pan, C., & Cheng, X. (2015). Modulation of fatty acid metabolism is involved in the alleviation of isoproterenol-induced rat heart failure by fenofibrate. *Molecular medicine reports*, 12(6), 7899–7906.
9. Wu, Y., Qin, Y. H., Liu, Y., Zhu, L., Zhao, X. X., Liu, Y. Y., Luo, S. W., Tang, G. S., & Shen, Q. (2019). Cardiac troponin I autoantibody induces myocardial dysfunction by PTEN signaling activation. *EBioMedicine*, 47, 329–340.
10. Yuan, S., Zhang, X., Zhan, J., Xie, R., Fan, J., Dai, B., Zhao, Y., Yin, Z., Liu, Q., Wang, D. W., Li, H., & Chen, C. (2024). Fibroblast-localized lncRNA CFIRL promotes cardiac fibrosis and dysfunction in dilated cardiomyopathy. *Science China. Life sciences*, 67(6), 1155–1169.
11. Ji, J. J., Qian, L. L., Zhu, Y., Jiang, Y., Guo, J. Q., Wu, Y., Yang, Z. W., Yao, Y. Y., & Ma, G. S. (2022). Kallistatin/Serpina3c inhibits cardiac fibrosis after myocardial infarction by regulating glycolysis via Nr4a1 activation. *Biochimica et biophysica acta. Molecular basis of disease*, 1868(9), 166441.
12. Khan, M. S., Shahid, I., Greene, S. J., Mentz, R. J., DeVore, A. D., & Butler, J. (2023). Mechanisms of current therapeutic strategies for heart failure: more questions than answers?. *Cardiovascular research*, 118(18), 3467–3481.
13. Boateng I. D. (2023). Ginkgols and bilobols in Ginkgo biloba L. A review of their extraction and bioactivities. *Phytotherapy research : PTR*, 37(8), 3211–3223.
14. Liu, Y., Xin, H., Zhang, Y., Che, F., Shen, N., & Cui, Y. (2022). Leaves, seeds and exocarp of Ginkgo biloba L. (Ginkgoaceae): A Comprehensive Review of Traditional Uses, phytochemistry, pharmacology, resource utilization and toxicity. *Journal of ethnopharmacology*, 298, 115645.

 doi:10.20944/preprints202504.0915.v1

15. Gong, G., Guan, Y. Y., Zhang, Z. L., Rahman, K., Wang, S. J., Zhou, S., Luan, X., & Zhang, H. (2020). Isorhamnetin: A review of pharmacological effects. *Biomedicine & pharmacotherapy = Biomedecine & pharmacotherapie*, 128, 110301.
16. Sun, J., Sun, G., Meng, X., Wang, H., Luo, Y., Qin, M., Ma, B., Wang, M., Cai, D., Guo, P., & Sun, X. (2013). Isorhamnetin protects against doxorubicin-induced cardiotoxicity in vivo and in vitro. *PloS one*, 8(5), e64526.
17. Zhao, T. T., Yang, T. L., Gong, L., & Wu, P. (2018). Isorhamnetin protects against hypoxia/reoxygenation-induced injure by attenuating apoptosis and oxidative stress in H9c2 cardiomyocytes. *Gene*, 666, 92–99.
18. Li, H. R., Zheng, X. M., Liu, Y., Tian, J. H., Kou, J. J., Shi, J. Z., Pang, X. B., Xie, X. M., & Yan, Y. (2022). L-Carnitine Alleviates the Myocardial Infarction and Left Ventricular Remodeling through Bax/Bcl-2 Signal Pathway. *Cardiovascular therapeutics*, 2022, 9615674.
19. Wang, J., Gong, H. M., Zou, H. H., Liang, L., & Wu, X. Y. (2018). Isorhamnetin prevents H2O2-induced oxidative stress in human retinal pigment epithelial cells. *Molecular medicine reports*, 17(1), 648–652.
20. Xu, J., Liang, S., Wang, Q., Zheng, Q., Wang, M., Qian, J., Yu, T., Lou, S., Luo, W., Zhou, H., & Liang, G. (2024). JOSD2 mediates isoprenaline-induced heart failure by deubiquitinating CaMKIIδ in cardiomyocytes. *Cellular and molecular life sciences : CMLS*, 81(1), 18.
21. Deglin, S. M., Deglin, J. M., & Chung, E. K. (1977). Drug-induced cardiovascular diseases. *Drugs*, 14(1), 29–40.
22. Oliver, E., Mayor, F., Jr, & D'Ocon, P. (2019). Beta-blockers: Historical Perspective and Mechanisms of Action. *Revista espanola de cardiologia (English ed.)*, 72(10), 853–862.
23. Pundir, S., Garg, P., Dviwedi, A., Ali, A., Kapoor, V. K., Kapoor, D., Kulshrestha, S., Lal, U. R., & Negi, P. (2021). Ethnomedicinal uses, phytochemistry and dermatological effects of Hippophae rhamnoides L.: A review. *Journal of ethnopharmacology*, 266, 113434.
24. Chen, T. L., Zhu, G. L., Wang, J. A., Zhang, G. D., Liu, H. F., Chen, J. R., Wang, Y., & He, X. L. (2015). Protective effects of isorhamnetin on apoptosis and inflammation in TNF-α-induced HUVECs injury. *International journal of clinical and experimental pathology*, 8(3), 2311–2320.
25. Xu, Y., Tang, C., Tan, S., Duan, J., Tian, H., & Yang, Y. (2020). Cardioprotective effect of isorhamnetin against myocardial ischemia reperfusion (I/R) injury in isolated rat heart through attenuation of apoptosis. *Journal of cellular and molecular medicine*, 24(11), 6253–6262.
26. Arden, N., & Betenbaugh, M. J. (2004). Life and death in mammalian cell culture: strategies for apoptosis inhibition. *Trends in biotechnology*, 22(4), 174–180.
27. Yang, B., Ye, D., & Wang, Y. (2013). Caspase-3 as a therapeutic target for heart failure. *Expert opinion on therapeutic targets*, 17(3), 255–263.
28. Pradelli, L. A., Bénéteau, M., & Ricci, J. E. (2010). Mitochondrial control of caspase-dependent and -independent cell death. *Cellular and molecular life sciences : CMLS*, 67(10), 1589–1597.
29. Wang, Y., Zhang, H., Chai, F., Liu, X., & Berk, M. (2014). The effects of escitalopram on myocardial apoptosis and the expression of Bax and Bcl-2 during myocardial ischemia/reperfusion in a model of rats with depression. *BMC psychiatry*, 14, 349.
30. Zhang, X., Wang, Q., Wang, X., Chen, X., Shao, M., Zhang, Q., Guo, D., Wu, Y., Li, C., Wang, W., & Wang, Y. (2019). Tanshinone IIA protects against heart failure post-myocardial infarction via AMPKs/mTOR-dependent autophagy pathway. *Biomedicine & pharmacotherapy = Biomedecine & pharmacotherapie*, 112, 108599.
31. Yan, Q., Liu, S., Sun, Y., Chen, C., Yang, S., Lin, M., Long, J., Yao, J., Lin, Y., Yi, F., Meng, L., Tan, Y., Ai, Q., Chen, N., & Yang, Y. (2023). Targeting oxidative stress as a preventive and therapeutic approach for cardiovascular disease. *Journal of translational medicine*, 21(1), 519.
32. Hou, X., Yang, S., & Yin, J. (2019). Blocking the REDD1/TXNIP axis ameliorates LPS-induced vascular endothelial cell injury through repressing oxidative stress and apoptosis. American journal of physiology. *Cell physiology*, 316(1), C104–C110.
33. Senoner, T., & Dichtl, W. (2019). Oxidative Stress in Cardiovascular Diseases: Still a Therapeutic Target?. *Nutrients*, 11(9), 2090.

 doi:10.20944/preprints202504.0915.v1

34. Chen, Q., Xu, Q., Zhu, H., Wang, J., Sun, N., Bian, H., Li, Y., & Lin, C. (2023). Salvianolic acid B promotes angiogenesis and inhibits cardiomyocyte apoptosis by regulating autophagy in myocardial ischemia. *Chinese medicine*, 18(1), 155.
35. Hosseini, A., Ghorbani, A., Alavi, M. S., Forouhi, N., Rajabian, A., Boroumand-Noughabi, S., Sahebkar, A., & Eid, A. H. (2023). Cardioprotective effect of Sanguisorba minor against isoprenaline-induced myocardial infarction in rats. *Frontiers in pharmacology*, 14, 1305816.
36. Liu, J., Li, X., Ding, L., Li, W., Niu, X., & Gao, D. (2023). GRK2 participation in cardiac hypertrophy induced by isoproterenol through the regulation of Nrf2 signaling and the promotion of NLRP3 inflammasome and oxidative stress. *International immunopharmacology*, 117, 109957.
37. Long, J., Gao, M., Kong, Y., Shen, X., Du, X., Son, Y. O., Shi, X., Liu, J., & Mo, X. (2012). Cardioprotective effect of total paeony glycosides against isoprenaline-induced myocardial ischemia in rats. *Phytomedicine : international journal of phytotherapy and phytopharmacology*, 19(8-9), 672–676.
38. Zhu, L., Wei, T., Chang, X., He, H., Gao, J., Wen, Z., & Yan, T. (2015). Effects of Salidroside on Myocardial Injury In Vivo In Vitro via Regulation of Nox/NF-κB/AP1 Pathway. *Inflammation*, 38(4), 1589–1598.
39. Maldonado, E., Rojas, D. A., Urbina, F., & Solari, A. (2021). The Use of Antioxidants as Potential Co-Adjuvants to Treat Chronic Chagas Disease. *Antioxidants (Basel, Switzerland)*, 10(7), 1022.
40. Bhatti, J. S., Bhatti, G. K., & Reddy, P. H. (2017). Mitochondrial dysfunction and oxidative stress in metabolic disorders - A step towards mitochondria based therapeutic strategies. Biochimica et biophysica acta. *Molecular basis of disease*, 1863(5), 1066–1077.
41. Peoples, J. N., Saraf, A., Ghazal, N., Pham, T. T., & Kwong, J. Q. (2019). Mitochondrial dysfunction and oxidative stress in heart disease. *Experimental & molecular medicine*, 51(12), 1–13.
42. Sinha, K., Das, J., Pal, P. B., & Sil, P. C. (2013). Oxidative stress: the mitochondria-dependent and mitochondria-independent pathways of apoptosis. Archives of toxicology, 87(7), 1157–1180.
43. Brown, D. A., & O'Rourke, B. (2010). Cardiac mitochondria and arrhythmias. *Cardiovascular research*, 88(2), 241–249.
44. Da Dalt, L., Cabodevilla, A. G., Goldberg, I. J., & Norata, G. D. (2023). Cardiac lipid metabolism, mitochondrial function, and heart failure. *Cardiovascular research*, 119(10), 1905–1914.
45. Yuan, H. J., Xue, Y. T., & Liu, Y. (2022). Cuproptosis, the novel therapeutic mechanism for heart failure: a narrative review. *Cardiovascular diagnosis and therapy*, 12(5), 681–692.
46. Abu Shelbayeh, O., Arroum, T., Morris, S., & Busch, K. B. (2023). PGC-1α Is a Master Regulator of Mitochondrial Lifecycle and ROS Stress Response. *Antioxidants (Basel, Switzerland)*, 12(5), 1075.
47. Montaigne, D., Butruille, L., & Staels, B. (2021). PPAR control of metabolism and cardiovascular functions. Nature reviews. *Cardiology*, 18(12), 809–823.
48. Qian, L., Zhu, Y., Deng, C., Liang, Z., Chen, J., Chen, Y., Wang, X., Liu, Y., Tian, Y., & Yang, Y. (2024). Peroxisome proliferator-activated receptor gamma coactivator-1 (PGC-1) family in physiological and pathophysiological process and diseases. *Signal transduction and targeted therapy*, 9(1), 50.
49. Ventura-Clapier, R., Garnier, A., & Veksler, V. (2008). Transcriptional control of mitochondrial biogenesis: the central role of PGC-1alpha. *Cardiovascular research*, 79(2), 208–217.
50. Chen, S., Zou, Y., Song, C., Cao, K., Cai, K., Wu, Y., Zhang, Z., Geng, D., Sun, W., Ouyang, N., Zhang, N., Li, Z., Sun, G., Zhang, Y., Sun, Y., & Zhang, Y. (2023). The role of glycolytic metabolic pathways in cardiovascular disease and potential therapeutic approaches. *Basic research in cardiology*, 118(1), 48.
51. Yang, T., Shu, X., Zhang, H. W., Sun, L. X., Yu, L., Liu, J., Sun, L. C., Yang, Z. H., & Ran, Y. L. (2020). Enolase 1 regulates stem cell-like properties in gastric cancer cells by stimulating glycolysis. *Cell death & disease*, 11(10), 870.